JACS
JOURNAL OF THE AMERICAN CHEMICAL SOCIETY

COMMUNICATION

pubs.acs.org/JACS

Five-Fold-Symmetric Macrocyclic Aromatic Pentamers: High-Affinity Cation Recognition, Ion-Pair-Induced Columnar Stacking, and Nanofibrillation

Changliang Ren,[†] Victor Maurizot,[‡] Huaiqing Zhao,[†] Jie Shen,[†] Feng Zhou,[§] Wei Qiang Ong,[†] Zhiyun Du,[∥] Kun Zhang,[∥] Haibin Su,[§] and Huaqiang Zeng*[,†]

[†]Department of Chemistry and NUS MedChem Program of the Office of Life Sciences, 3 Science Drive 3, National University of Singapore, Singapore 117543

[‡]CNAB—UMR5084, Université de Bordeaux, UMR CNRS 5248, Institute Européen de Chimie et Biologie, 2 rue Robert Escarpit, 33607 Pessac Cedex, France

[§]Division of Materials Science, 50 Nanyang Avenue, Nanyang Technological University, Singapore 639798

[∥]Faculty of Light Industry and Chemical Engineering, Guang Dong University of Technology, Guang Dong 510006, China

Supporting Information

ABSTRACT: Described in this study is a conceptually new class of five-fold-symmetric cavity-containing planar pentameric macrocycles with their interior decorated by five convergently aligned, properly spaced carbonyl oxygen atoms. These cation-binding oxygens enclose a hydrophilic lumen of 2.85 Å in radius and thus display high-affinity binding toward alkali metal cations, and possibly many other cations, too. Arising from their high-affinity recognition of metal ions, these planar macrocycles form cation- or ion-pair-induced one-dimensional columnar aggregates, and subsequently fascinating fibrillation results.

One-dimensional (1D) fibers or nanotubes assembled from organic molecules are promising materials[1] for applications as diverse as nanodevices,[1b,c,g,h] sensors,[2a−c] and water transporters.[2d] These organic columnar aggregates are predominantly stabilized by hydrogen-bonding or $\pi-\pi$ stacking forces, or a combination of both.[1a−h,2e−2m] Although metal ions can offer unique properties and geometries for functional diversification, metal−ligand coordination bonds have received comparatively much less attention in the construction of fibrillar materials[3a] derived from acyclic or macrocyclic organic molecules.[1i−k] On the other hand, macrocyclic molecules suitable for constructing metal-containing 1D materials are particularly limited and mostly rely on a G-quartet and its derivatives,[1i,3b−3d] Schiff base macrocycles,[3e−h] and porphyrin and its analogues.[3h−m] Moreover, these fibrillar ensembles are largely cation-mediated, where cations either are sandwiched between macrocycles[1i,3b,3d−3f] or form additional coordination bonds directly and vertically with the neighboring macrocyclic ligands,[3h−m] while ion-pair-induced 1D columnar aggregation[3g] is very scarce. We report here a new class of planar five-fold-symmetric macrocyclic pentamers whose appropriately sized interiors are decorated by five carbonyl oxygens that display high-affinity binding toward alkali metal ions through metal−oxygen interatomic interactions. Cation- or scarcely reported ion-pair-induced fibrillation thus results from these high-affinity bindings and planar geometries.

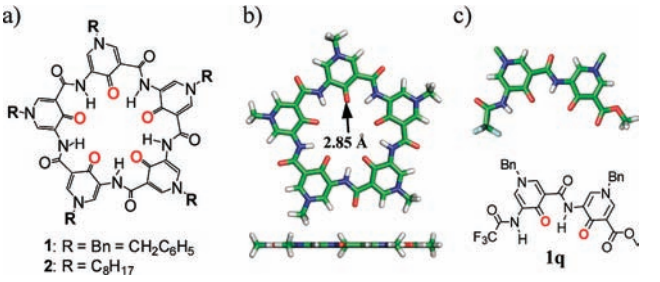

Figure 1. (a) Chemical structures of pentamers **1** and **2**. (b) Top and side views of computationally optimized structures for **1** and **2**, with the exterior side chains replaced by methyl groups at the B3LYP/6-31G* level, illustrating five-fold-symmetric planarity in **1** and **2**. (c) Chemical and crystal structures of dimer **1q**.

As illustrated in Figure 1a, pentameric molecules **1** and **2** are made of five alkylated 4(1*H*)-pyridone motifs meta-linked by secondary amide groups. Both carbonyl oxygens and amide protons point inward to form a continuous intramolecularly H-bonded network in a way such that the H-bonding rigidified backbone becomes increasingly curved and eventually cyclizable to arrive at a pentagon shape.[4] *Ab initio* calculation at the B3LYP/6-31G* level (Figure 1b) on pentamers **1** and **2** shows that such a pentagon shape encloses a hydrophilic oxygen-containing cavity of 2.85 Å, nearly identical to the average coordination bond distance between K^+ ions and covalently bound oxygen atoms.[5a] These convergently aligned, properly spaced oxygens should therefore suggest high-affinity cooperative recognition of the alkali metal ions by pentameric molecules **1** and **2**. Additionally, the planar geometry in **1** and **2** should promote the formation of cation- or ion-pair-mediated 1D stacked structures under suitable conditions.

Pentamers **1** and **2** were both made by a stepwise construction strategy using HBTU-mediated amide coupling requiring 15−16 steps with an overall yield of 1−2%, starting from the commercially available diethyl 3-oxopentanedioate (Schemes S1 and S2[5b]). Their identity was unambiguously confirmed by excellent

Received: July 12, 2011
Published: August 08, 2011

Table 1. K_a, R, and ΔG^o for 2 Complexing Alkali Picrate Salts from Li^+ to Cs^+ in $H_2O/CHCl_3$ at 25 °C, Obtained by Cram's Method[5c]

picrate salt, M	R^a	K_a ($\times 10^8$ M^{-1})^b	$-\Delta G°$ (kcal/mol)
Li^+	0.719	2.28 ± 0.10	11.35
Na^+	0.715	1.78 ± 0.09	11.20
K^+	0.645	0.57 ± 0.04	10.53
Rb^+	0.615	0.24 ± 0.03	10.01
Cs^+	0.602	0.18 ± 0.01	9.84

[a] [Guest]/[host] ratio in $CHCl_3$ layer at equilibrium. [b] Averaged values over three runs with the assumption of 1:1 guest/host binding stoichiometry.[4e,5d]

matching between their experimentally obtained high-resolution masses and the calculated ones;[5b] their highly symmetrical nature was revealed by their highly simplified ^{1}H NMR spectra at 110 °C in DMSO-d_6 for **1** and 33% $CDCl_3$/67% DMSO-d_6 for **2** that showed three sets of proton signals corresponding to protons on the pyridone motif and amide bonds.[5b] The crystal structure of dimer molecule **1q** demonstrates the ability of the interior carbonyl oxygen to form intramolecular H-bonds (2.00−2.27 Å) with the amide proton, restricting the conformational freedom of the amide bond and biasing the aromatic backbone into a crescent shape (Figures 1c and S2).[5e]

An indication suggesting good binding of alkali metal ions by **1** and **2** came from the solubility test: **1** is sparingly soluble in DMSO (<0.01 mM at room temperature), but addition of 1 equiv of alkali metal ions of their tetraphenylborate (BPh_4) salts from Li^+ to Cs^+ invariably dissolves >20 mM **1** into DMSO at room temperature. Following Cram's method using picrate extraction experiments at 10 mM,[5b,c] the association constants (K_a) for complexation of **2** to five alkali metal ions were evaluated in a $H_2O/CHCl_3$ system. The data compiled in Table 1 show high-affinity binding of $\sim 10^8$ M^{-1} with a good degree of selectivity toward alkali ions by **2**. The strong binding between **2** and alkali metal ions is established further by being able to detect the complex formation using thin-layer chromatography (TLC). In the presence of 5 equiv of $KBPh_4$ salt, **2** mostly exists in the complex form in TLC plates; free **2** is very minimal (lanes 7 and 8, Figure S3). This trend persists when 5 equiv of other $MBPh_4$ salts (M = Li^+, Na^+, Rb^+ and Cs^+) were used.

The high-affinity binding exhibited by **2** led us to explore the possibility of **2** stabilizing the columnar stacking in the presence of alkali ions (Li^+, Na^+, K^+, Rb^+, and Cs^+). This was first investigated by high-resolution ESI mass spectroscopy. In addition to the 1:1 complex $[\mathbf{2}\cdot M]^+$, other aggregated species, such as $[\mathbf{2}_2\cdot M]^+$, $[\mathbf{2}_3\cdot M_2]^{2+}$, $[\mathbf{2}_4\cdot M_3]^{3+}$ (M = Li^+, Na^+, K^+, Rb^+, and Cs^+) and $[\mathbf{2}_2\cdot Li_2\cdot H_2O]^{2+}$, were observed (Figures S4−S8) Most noteworthy is the strongest tendency of **2** to aggregate in the presence of Cs^+, predominantly forming a sandwiched $[\mathbf{2}_3\cdot Cs_2]^{2+}$ species with an almost complete disappearance of the 1:1 complex $[\mathbf{2}\cdot Cs]^+$. This finding is consistent with the experimental observation of Cs^+-mediated fiber formation (Table 2 and Figures 2 and 3) and with *ab initio* molecular modeling (B3LYP/6-31G*, Figure S9), showing that Cs^+ ions, being largest in size, are more capable of forming and stabilizing sandwiched assemblies with respect to other ions.

To enable direct visualization of the solid-state morphologies resulting from molecular interactions between alkali ions and **1** or **2**, and subsequent intercolumnar associations, transmission electron microscopy (TEM) was employed. In a typical experiment, MeOH in the case of **1** or $CHCl_3$ in the case of **2** was slowly diffused over a few days or weeks into an acetonitrile solution containing a 1:1 ratio of pentamer (**1** or **2**) and the respective $MBPh_4$ salt (M = Li^+, Na^+, K^+, Rb^+, and Cs^+) at 10 mM. The slowly formed aggregates were spotted onto TEM grids and examined by TEM. TEM images (Figures 2 and S10−S12) reveal that, except for $KBPh_4$, **1** forms fibers with all the other four metal ions and that, for **2**, appreciable fibers can be observed only for $RbBPh_4$ and $CsBPh_4$. In other words, **1** carrying benzyl side chains forms good fibers with $MBPh_4$ salts more often than **2** carrying octyl side chains (Table 2). This is consistent with the theoretical calculations, revealing the existence of extensive intermolecular H-bonds among stacked molecules of **1** (Figure S31) that increases the stability of 1D columnar stack.

The potential to use ion-pairs to induce fiber formation of **1** or **2** was also investigated by TEM. A total of 10 salts (MCl and MBr, where M = Li^+, Na^+, K^+, Rb^+, and Cs^+) were tested against both **1** and **2**. Akin to the case of $MBPh_4$, examining these 20 combinations (Table 2, Figures 2 and S13−S17) highlights a similar trend: **1** forms fibers with alkali halide salts more often than **2**. Aside from the fibers seen in the majority of cases, defined nanorods and nanoropes (Figure 2) were also produced when **2** was mixed with LiCl, NaBr, and KBr, and possibly with LiBr (Figure S11). For instance, KBr salts combine with **2** to produce well-defined nanorods, typically measuring 50−200 nm in width and 1−3 μm in length, and **2** in the presence of NaBr salts assembles into very flexible, easily coiled, and virtually endless nanoropes, each with a uniform diameter from 0.2 to 1 μm (Figures 2 and S14).

Energy-dispersive X-ray analysis (EDX), a microanalytical technique for elemental mapping, was carried out in an effort to identify elements present in the above-formed fibers. Selective EDX analyses on four types of as-produced fibers formed between **1** and $CsBPh_4$ or KCl, and between **2** and NaBr or KBr, reveal the elemental occurrence of Cs, K/Cl, Na/Br, and K/Br in these fibers, respectively, unambiguously confirming their incorporation into the fibers (Figures S18, S19, S21, S23, and S24).

To gain further insights into the above-formed 1D stacked structures at the molecular level, *ab initio* theoretical investigations at

Table 2. Cation- and ion pair-induced fibrillation[a] of 1 or 2 in the presence of various alkali metal salts.

host	alkali $MBPh_4$ salts				alkali MX Salts									
	Li^+	Na^+	Rb^+	Cs^+	LiCl	LiBr	NaCl	NaBr	KCl	KBr	RbCl	RbBr	CsCl	CsBr
1	yes	yes	yes[c]	yes	yes[b]	yes	yes	yes	yes[b]	yes[b]	yes	—[e]	yes[b]	—[f]
2	—[e]	—[e]	yes	yes	nanorod[d]	nanorod[c,d]	—[e]	nanorope[b]	yes	nanorod[b]	—[e]	yes	yes[b]	yes[c]

[a] Obtained by slow diffusion of ethyl acetate into **1**-containing DMSO solution, or MeOH into **2**-containing $CHCl_3$ solution; in some cases, a tiny amount of H_2O was added to dissolve the salts. In all the salts studied, only $KBPh_4$ does not induce any noticeable fiber formation. [b] High quality with smooth surfaces. [c] Moderate or bad quality. [d] Irregular shapes. [e] No significant fibers were observed. [f] A mixture of irregular nanorods and fibers.

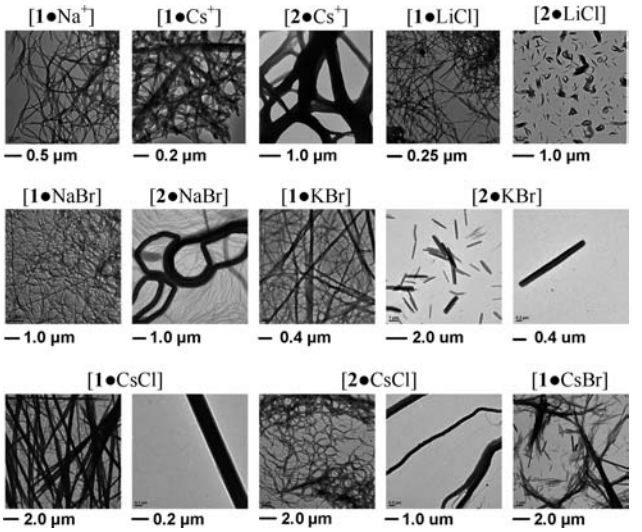

Figure 2. Selected TEM images illustrating the fibrillation induced by alkali metal salts $M^+BPh_4^-$ and ion pairs M^+X^-. Fibers were obtained by slow diffusion of ethyl acetate into **1**-containing DMSO solution, or MeOH into **2**-containing $CHCl_3$ solution; in some cases, a tiny amount of H_2O was added to dissolve the salts.

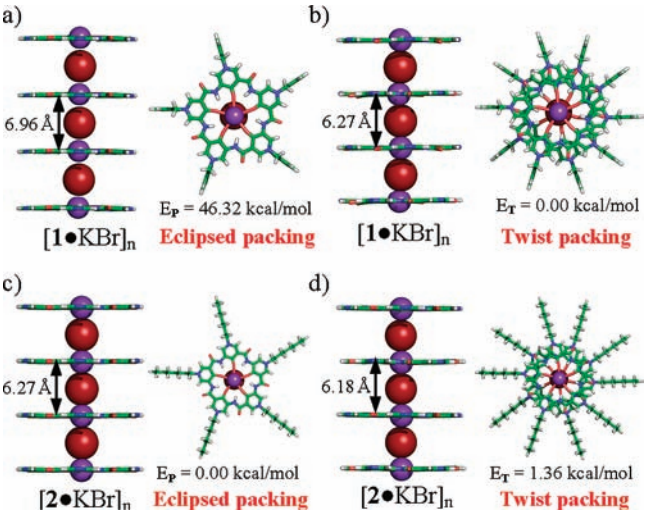

Figure 3. Computationally optimized structures of 1D columnar aggregates possibly formed by (a,b) $[\mathbf{1}\cdot KBr]_n$ and (c,d) $[\mathbf{2}\cdot KBr]_n$ at the B3LYP/6-31G* level under periodic boundary conditions. The top-down views illustrate two possible packing modes and their relative energies. Side views ,with the exterior side chains removed, illustrate the interplanar distances that dictate the strength of ionic interactions. In the CPK models, K^+ = 1.38 Å and Br^- = 1.95 Å.

the B3LYP/6-31G* level under periodic boundary conditions were carried out for 1D columns formed between KBr and **1** or **2** (Figure 3). Two packing modes may develop in forming 1D columns: in the eclipsed mode, pentamers are vertically aligned and superimposable over each other (Figure 3a,c); in the twist mode, vertically adjacent pentamers are twisted by 32−33° so that the steric hindrance, if any, among exterior side chains can be possibly released (Figure 3b,d). For **1**, the eclipsed mode (Figure 3a) is energetically less stable than the twist mode (Figure 3b) by 46.32 kcal/mol. This enhanced stability results from (1) the sterically very bulky benzyl side chains that lessen the ionic interactions among K^+ and Br^- ions, as evidenced by the larger interplanar separation of 6.96 Å in the eclipsed mode with respect to 6.27 Å in the twist mode, and (2) intermolecular H-bonds (2.20 Å) formed between one of the aromatic protons from every exterior benzyl group and the amide carbonyl oxygen that is right below it (Figure S31). For **2**, the difference in relative energy between the eclipsed and twist modes is quite small, and the eclipsed packing mode (Figure 3c) is marginally more stable than the twist mode (Figure 3d), by 1.32 kcal/mol. This is a result of an increase in favorable hydrophobic interactions and essentially an absence of steric hindrance among exterior octyl side chains, which can more than compensate the lessened ionic interactions (6.27 Å, Figure 3c) in the eclipsed packing mode as compared to the twist mode (6.18 Å, Figure 3c). Overall, the computationally obtained more stable structures (Figure 3b,c) show that K^+ cations stay in the center of the cavity and are stabilized by the closest five carbonyl oxygen atoms. Cross-linking the planar pentameric molecules to form a 1D stacked Br^--sandwiched supramolecular ensemble was achieved by stabilizing ionic interactions between K^+ and Br^-, whereby the interplanar distance of 6.27 Å (Figure 3b,c) is 0.39 Å less than twice the sum of the van der Waals radii of K^+ (vdW = 1.38 Å) and Br^- (vdW = 1.95 Å). These 1D aggregates are further stabilized by intermolecular H-bonds between aromatic benzyl protons and amide carbonyl oxygen atoms in **1**, and by hydrophobic side-chain interactions in **2**.

The formation of ion-pair-induced 1D columnar structures can be supported by the exchange experiments,[5b] where fibers formed from **1** and KCl or KBr, i.e., $\mathbf{1}\cdot$KCl or $\mathbf{1}\cdot$KBr fibers, were suspended in MeOH solution and treated respectively with a large excess of tetrabutylammonium bromide (TBABr) or TBACl. If the anions (Cl^- and Br^-) occupy the intercolumnar spaces, where these loosely bound anions are separated from the cations by >12 Å on the basis of the dimensionality of **1**, presumably they should remain exchangeable, largely to equal extents, respectively, by excessive Br^- and Cl^- anions. The exchange experiments, however, show that ∼91−96% Cl^- anions trapped in the $\mathbf{1}\cdot$KCl fibers can be exchanged by excessive Br^- anions (Figure S20), while only ∼26−30% Br^- anions in the $\mathbf{1}\cdot$KBr fibers remains exchangeable by excessive Cl^- anions (Figure S22). These experiments suggest that anions stay inside the column and that KBr stabilizes the 1D fibrillar structures formed from **1** better than KCl. Consistent with these data, (1) TEM images reveal significant morphological changes for $\mathbf{1}\cdot$KCl fibers after exchange with TBABr (Figures S25 vs S26) and little change in morphology in $\mathbf{1}\cdot$KBr fibers after exchange with TBACl (Figures S27 vs S28), and (2) powder X-ray diffraction (XRD) analyses show that the dominant peak at the lower angle ($2\theta < 5°$) from the $\mathbf{1}\cdot$KCl fibers after exchange with KBr (Figure S30) is closer to that of the $\mathbf{1}\cdot$KBr fibers (Figure S15) than that of the $\mathbf{1}\cdot$KCl fibers (Figure S29). By allowing anions to sit inside the columns and between cations, the 1D fibrillar structures should become more stable due to the existence of favorable ionic interactions and a concurrent reduction in electrostatic repulsions occurring among cations from the vertically aligned adjacent macrocycles if anions are to occupy the intercolumnar spaces.

The inference on the intercolumnar association was achieved by carrying out XRD analyses, revealing a possible hexagonal arrangement involving 1D columns for the fibers prepared from **1** in the presence of $LiBPh_4$ (Figure S10), $NaBPh_4$ (Figure S10), LiBr (Figure S13), NaCl (Figure S14), NaBr (Figure S14), and KCl (Figure S15). As an example, the X-ray diffractogram of

1·NaCl fibers (Figure S14) shows a strong peak at d_{100} = 19.98 Å (2θ = 4.42°), along with two deconvoluted weaker peaks at d_{110} = 10.91 Å and d_{200} = 9.75 Å, possibly indicating a hexagonal lattice with an intercolumnar distance of d_{hex} = 23.07 Å. Compared to the overall radius of 1.18 nm, inclusive of 0.68 nm from its pentamer core and 0.50 nm from the benzyl side chains for the 1D columns formed from **1** (Figure 3b), the overlap among the 1D columns is ~0.05 nm, suggesting that the exterior benzyl side chains in the twist packing mode (Figure 3b) do not penetrate into each other, which is consistent with the rigid nature of benzyl groups. Assuming formation of a hexagonal lattice, the calculated intercolumnar distances of 2.24−2.44 nm indicate an overlap of <0.12 nm for the **1**·LiBr, **1**·NaBr, and **1**·KCl fibers (Figures S13−S15) and no overlap for the **1**·$LiBPh_4$ and **1**·$NaBPh_4$ fibers (Figure S10). Similar XRD analyses (Figures S10−S17) on other fibers formed from **1** or **2** (Table 1) give inconclusive information on the intercolumnar arrangement of 1D columns.

In summary, we have developed an entirely new class of cation-binding foldamer-based pentameric macrocycles capable of high-affinity recognition of metal ions and self-assembling into tunable 1D columnar aggregates that further associate to form unusual cation-containing or ion-pair-induced fibers of varying shapes and sizes, controllable by alkali metal ions or their halide salts. The modular nature of the described macrocycles also enables easy modification of the outer surfaces, and, in combination with other monomeric building blocks recently reported by us,[4e] further allows the interior properties to be finely tuned with respect to both ion-binding affinity and selectivity. Accordingly, an enriched family of closely related, appropriately designed structural variations can be envisioned for some interesting applications.[1−3,4e,6]

■ ASSOCIATED CONTENT

Supporting Information. Procedures and characterization data. This material is available free of charge via the Internet at http://pubs.acs.org.

■ AUTHOR INFORMATION

Corresponding Author
chmzh@nus.edu.sg

■ ACKNOWLEDGMENT

We thank National University of Singapore AcRF Tier 1 Grants (R-143-000-375-112 and R-143-000-398-112 to H.Z.).

■ REFERENCES

(1) (a) Bong, D. T.; Clark, T. D.; Granja, J. R.; Ghadiri, M. R. *Angew. Chem., Int. Ed.* **2001**, *40*, 988. (b) Schenning, A. P. H. J.; Meijer, E. W. *Chem. Commun.* **2005**, 3245. (c) Wu, J.; Pisula, W.; Mullen, K. *Chem. Rev.* **2007**, *107*, 718. (d) Zang, L.; Che, Y.; Moore, J. S. *Acc. Chem. Res.* **2008**, *41*, 1596. (e) Palmer, L. C.; Stupp, S. I. *Acc. Chem. Res.* **2008**, *41*, 1674. (f) Zhao, Y. S.; Fu, H. B.; Peng, A. D.; Ma, Y.; Liao, Q.; Yao, J. N. *Acc. Chem. Res.* **2010**, *43*, 409. (g) Zayed, J. M.; Nouvel, N.; Rauwald, U.; Scherman, O. A. *Chem. Soc. Rev.* **2010**, *39*, 2806. (h) Brea, R. J.; Reiriz, C.; Granja, J. R. *Chem. Soc. Rev.* **2010**, *39*, 1448. (i) Davis, J. T.; Spada, G. P. *Chem. Soc. Rev.* **2007**, *36*, 296. (j) Beletskaya, I.; Tyurin, V. S.; Tsivadze, A. Y.; Guilard, R.; Stern, C. *Chem. Rev.* **2009**, *109*, 165. (k) Hui, J. K. H.; MacLachlan, M. J. *Coord. Chem. Rev.* **2010**, *254*, 2363. (l) Ajayaghosh, A.; Chithra, P.; Varghese, R. *Angew. Chem., Int. Ed.* **2007**, *46*, 230. (m) Ajayaghosh, A.; Chithra, P.; Varghese, R.; Divya, K. P. *Chem. Commun.* **2008**, 969.

(2) (a) Hughes, A. D.; Glenn, I. C.; Patrick, A. D.; Ellington, A.; Anslyn, E. V. *Chem.—Eur. J.* **2008**, *14*, 1822. (b) Che, Y. K.; Yang, X. M.; Loser, S.; Zang, L. *Nano Lett.* **2008**, *8*, 2219. (c) Yin, M.; Shen, J.; Pisula, W.; Liang, M.; Zhi, L.; Mullen, K. *J. Am. Chem. Soc.* **2009**, *131*, 14618. (d) Kaucher, M. S.; Peterca, M.; Dulcey, A. E.; Kim, A. J.; Vinogradov, S. A.; Hammer, D. A.; Heiney, P. A.; Percec, V. *J. Am. Chem. Soc.* **2007**, *129*, 11698. (e) Reches, M.; Gazit, E. *Science* **2003**, *300*, 625. (f) Hill, J. P.; Jin, W.; Kosaka, A.; Fukushima, T.; Ichihara, H.; Shimomura, T.; Ito, K.; Hashizume, T.; Ishii, N.; Aida, T. *Science* **2004**, *304*, 1481. (g) Balakrishnan, K.; Datar, A.; Zhang, W.; Yang, X.; Naddo, T.; Huang, J.; Zuo, J.; Yen, M.; Moore, J. S.; Zang, L. *J. Am. Chem. Soc.* **2006**, *128*, 6576. (h) Stępień, M.; Donnio, B.; Sessler, J. *Angew. Chem., Int. Ed.* **2007**, *46*, 1431. (i) Chen, Y. L.; Zhu, B.; Zhang, F.; Han, Y.; Bo, Z. S. *Angew. Chem., Int. Ed.* **2008**, *47*, 6015. (j) Xu, Y. X.; Zhao, X.; Jiang, X. K.; Li, Z. T. *Chem. Commun.* **2009**, 4212. (k) Hisaki, I.; Shigemitsu, H.; Sakamoto, Y.; Hasegawa, Y.; Okajima, Y.; Nakano, K.; Tohnai, N.; Miyata, M. *Angew. Chem., Int. Ed.* **2009**, *48*, 5465. (l) Fischer, L.; Decossas, M.; Briand, J. P.; Didierjean, C.; Guichard, G. *Angew. Chem., Int. Ed.* **2009**, *48*, 1625. (m) Raghavender, U. S.; Kantharaju; Aravinda, S.; Shamala, N.; Balaram, P. *J. Am. Chem. Soc.* **2010**, *132*, 1075.

(3) (a) Ghosh, S.; Mukherjee, A.; Sadler, P. J.; Verma, S. *Angew. Chem., Int. Ed.* **2008**, *47*, 2217. (b) Davis, J. T. *Angew. Chem., Int. Ed.* **2004**, *43*, 668. (c) Garciaa-Arriaga, M.; Hobley, G.; Rivera, J. M. *J. Am. Chem. Soc.* **2008**, *130*, 10492. (d) González-Rodríguez, D.; Dongen, J. L. J. v.; Lutz, M.; Spek, A. L.; Schenning, A. P. H. J.; Meijer, E. W. *Nat. Chem.* **2009**, *1*, 151. (e) Gallant, A. J.; MacLachlan, M. J. *Angew. Chem., Int. Ed.* **2003**, *42*, 5307. (f) Akine, S.; Utsuno, F.; Nabeshima, T. *Chem. Commun.* **2010**, *46*, 1029. (g) Yamamura, M.; Sasaki, M.; Kyotani, M.; Orita, H.; Nabeshima, T. *Chem.—Eur. J.* **2010**, *16*, 10638. (h) Hui, J. K. H.; Yu, Z.; MacLachlan, M. J. *Angew. Chem., Int. Ed.* **2007**, *46*, 7980. (i) Wang, Z.; Medforth, C. J.; Shelnutt, J. A. *J. Am. Chem. Soc.* **2004**, *126*, 15954. (j) Shirakawa, M.; Fujita, N.; Shinkai, S. *J. Am. Chem. Soc.* **2005**, *127*, 4164. (k) Koepf, M.; Wytko, J. A.; Bucher, J.-P.; Weiss, J. *J. Am. Chem. Soc.* **2008**, *130*, 9994. (l) Frischmann, P. D.; Guieu, S.; Tabeshi, R.; MacLachlan, M. J. *J. Am. Chem. Soc.* **2010**, *132*, 7668. (m) Iavicoli, P. *et al J. Am. Chem. Soc.* **2010**, *132*, 9350.

(4) This is an intrinsic feature of certain classes of foldamer molecules: (a) Qin, B.; Chen, X. Y.; Fang, X.; Shu, Y. Y.; Yip, Y. K.; Yan, Y.; Pan, S. Y.; Ong, W. Q.; Ren, C. L.; Su, H. B.; Zeng, H. Q. *Org. Lett.* **2008**, *10*, 5127. (b) Yan, Y.; Qin, B.; Shu, Y. Y.; Chen, X. Y.; Yip, Y. K.; Zhang, D. W.; Su, H. B.; Zeng, H. Q. *Org. Lett.* **2009**, *11*, 1201. (c) Yan, Y.; Qin, B.; Ren, C. L.; Chen, X. Y.; Yip, Y. K.; Ye, R. J.; Zhang, D. W.; Su, H. B.; Zeng, H. Q. *J. Am. Chem. Soc.* **2010**, *132*, 5869. (d) Zhang, Z.; Xia, B.; Han, C.; Yu, Y.; Huang, F. *Org. Lett.* **2010**, *12*, 3285. (e) Qin, B.; Ren, C. L.; Ye, R. J.; Sun, C.; Chiad, K.; Chen, X. Y.; Li, Z.; Xue, F.; Su, H. B.; Chass, G. A.; Zeng, H. Q. *J. Am. Chem. Soc.* **2010**, *132*, 9564. (f) Guieu, S.; Crane, A. K.; MacLachlan, M. J. *Chem. Commun.* **2011**, *47*, 1169. (g) Qin, B.; Ong, W. Q.; Ye, R. J.; Du, Z. Y.; Chen, X. Y.; Yan, Y.; Zhang, K.; Su, H. B.; Zeng, H. Q. *Chem. Commun.* **2011**, *47*, 5419. (h) Qin, B.; Sun, C.; Liu, Y.; Shen, J.; Ye, R. J.; Zhu, J.; Duan, X.-F.; Zeng, H. Q. *Org. Lett.* **2011**, *13*, 2270.

(5) (a) Bajaj, A. V.; Poonia, N. S. *Coord. Chem. Rev.* **1988**, *87*, 55. (b) See the Supporting Information. (c) Moore, S. S.; Tarnowski, T. L.; Newcomb, M.; Cram, D. J. *J. Am. Chem. Soc.* **1977**, *99*, 6398.(d) As shown in Figure S9, computationally, cations are located within the cavity and essentially coplanar with the pentameric backbone of **1** or **2**, making it unlikely for one pentamer molecule to simutaneouly bind two cations due to the repulsion between the two cations in proximity. (e) The partially refined structure of pentamer **1** does reveal five-fold symmetry and a nearly planar backbone in **1** (Figure S1).

(6) (a) Zhu, Y. Y.; Li, C.; Li, G. Y.; Jiang, X. K.; Li, Z. T. *J. Org. Chem.* **2008**, *73*, 1745. (b) Sanford, A. R.; Yuan, L.; Feng, W.; Yamato, K.; Flowersb, R. A.; Gong, B. *Chem. Commun.* **2005**, 4720. (c) Helsel, A. J.; Brown, A. L.; Yamato, K.; Feng, W.; Yuan, L. H.; Clements, A. J.; Harding, S. V.; Szabo, G.; Shao, Z. F.; Gong, B. *J. Am. Chem. Soc.* **2008**, *130*, 15784. (d) Shirude, P. S.; Gillies, E. R.; Ladame, S.; Godde, F.; Shin-Ya, K.; Huc, I.; Balasubramanian, S. *J. Am. Chem. Soc.* **2007**, *129*, 11890.